

Cite this: DOI: 10.1039/c3gc40267c

# Metal-containing zeolites as efficient catalysts for the transformation of highly valuable chiral biomass-derived products

Cecilia Paris, Manuel Moliner\* and Avelino Corma\*

Received 5th February 2013,  
Accepted 22nd May 2013

DOI: 10.1039/c3gc40267c

www.rsc.org/greenchem

Metal-containing zeolites, especially Sn-Beta, perform as very efficient heterogeneous catalysts in the selective oxidation of levoglucosenone, which is considered as a platform chemical for the production of highly-valuable chemicals, towards the synthesis of the optically pure  $\gamma$ -lactone (*S*)- $\gamma$ -hydroxymethyl- $\alpha,\beta$ -butenolide (HBO) using  $\text{H}_2\text{O}_2$  as an oxidizing agent. Using Sn-Beta as a catalyst, yields up to 75% of (*S*)- $\gamma$ -hydroxymethyl- $\alpha,\beta$ -butenolide are achieved in a "one-pot" cascade reaction. When Sn-Beta is combined with an acid resin, such as Amberlyst-15, the "two-step" process allows yields up to 90%.

## 1. Introduction

In order to reduce the current dependence on fossil fuels, there is growing interest in renewable sources. Indeed, a great deal of efforts have been made in the last few decades to develop efficient methods to produce valuable chemicals from biomass, offering alternative routes besides traditional synthetic pathways.<sup>1</sup> In this context, lignocellulosic biomass has become one of the most sustainable carbon supplies for producing valuable chemicals, and particularly, catalytic fast pyrolysis (CFP) of this lignocellulosic biomass has been deeply studied in order to maximize the yield towards target products.<sup>2</sup> The pyrolysis oil product composition highly depends on the biomass source, the catalyst and the reaction conditions used.<sup>2</sup>

Levoglucosenone (LGO) is one of the most interesting valuable products that can be obtained from CFP. LGO is a dehydrated sugar presenting two chiral and six different functional carbon atoms, and it has been intensively used in the organic synthesis of several chemical compounds, such as natural products, nucleosides, anticancer drugs, and building blocks.<sup>3</sup> It has been reported that the acid-catalyzed pyrolysis process allows increasing the selectivity towards LGO (up to 30%), using glucose, cellulose or birch and pine wood as biomass sources, and phosphoric acid as a catalyst.<sup>4</sup> In addition, the use of zeolites as acid catalysts in the CFP process has permitted to enhance the LGO selectivity up to

40% of the produced oxygenated products, while increasing at the same time the production of other highly-valuable oxygenated products, such as furfural.<sup>5</sup> In this sense, the ability to increase the selectivity towards target products would make feasible the production of those key products from pyrolysis oils. Interestingly, a new and feasible procedure has been recently reported for recovering LGO from pyrolytic liquids by distillation.<sup>6</sup>

LGO and related products, such as levoglucosan, are considered the platform chemicals for the production of several valuable products (see Fig. 1).<sup>7</sup> From the different possible reaction pathways using LGO as a precursor, its oxidation towards the unsaturated chiral  $\gamma$ -lactone (*S*)- $\gamma$ -hydroxymethyl- $\alpha,\beta$ -butenolide (HBO in Fig. 1) is especially interesting since HBO is used in the synthesis of many drugs (such as Burseran or Isostegane),<sup>8</sup> aromatisers<sup>9</sup> and antiviral agents against the human immunodeficiency virus (HIV) or hepatitis B virus.<sup>10</sup>

The most efficient method described for the synthesis of HBO was reported by Koseki *et al.*<sup>11</sup> Butenolide HBO is obtained from LGO by following a two-step procedure. First, LGO is oxidized using organic peracids (such as peracetic acid or *m*-chloroperbenzoic acid) in acetic acid during 48 hours, obtaining the intermediate formate lactone (FBO, see Fig. 2). Second, the reaction mixture is concentrated *in vacuo*, and methanol and HCl were added to convert formate lactone FBO into the butenolide HBO. The reaction occurs through a Baeyer-Villiger oxidation, as Shafizadeh *et al.* demonstrated using different spectroscopic data.<sup>12</sup>

Corma *et al.* first synthesized Sn-Beta, as a high silica zeolite with Beta structure containing tetrahedrally coordinated isolated tin centers.<sup>13</sup> This zeolitic material

Instituto de Tecnología Química (UPV-CSIC), Universidad Politécnica de Valencia, Consejo Superior de Investigaciones Científicas, Valencia, 46022, Spain.  
E-mail: acorma@itq.upv.es, mmoliner@itq.upv.es

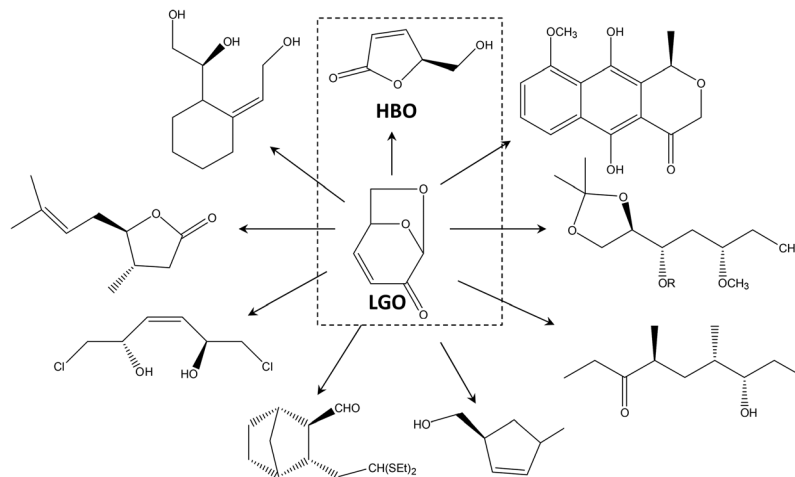


Fig. 1 Different reaction pathways of levoglucosenone.

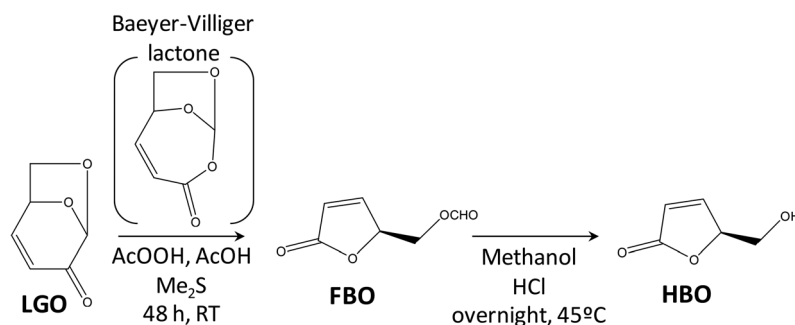


Fig. 2 The described reaction pathway for the oxidation of levoglucosenone to unsaturated  $\gamma$ -lactone (*S*)- $\gamma$ -hydroxymethyl- $\alpha,\beta$ -butenolide (HBO).

performs as a heterogeneous green oxidation catalyst using hydrogen peroxide, and shows excellent product selectivities in the Baeyer–Villiger or Meerwein–Ponndorf–Verley (MPV) reactions.<sup>14</sup> It has been demonstrated by theoretical calculations that the isolated tin centers in the zeolite framework act as Lewis acid sites, showing strong interactions with the carbonyl/hydroxyl moieties of reactants.<sup>15</sup>

Recently, Sn-Beta has been used for biomass transformations, since many biomass routes present molecules containing carbonyl groups, requiring selective catalysts capable to activate those carbonyl functionalities to direct different reaction pathways.<sup>16</sup> Indeed, Sn-Beta has been applied as a very efficient heterogeneous catalyst for the isomerization of sugars,<sup>17</sup> conversion of sugars to furfural-based heterocycles,<sup>18</sup> conversion of sugars to lactic acid derivatives,<sup>19</sup> and epimerization of sugars for the synthesis of rare monosaccharides.<sup>20</sup>

Herein, we will use Sn-Beta, and related metal-containing zeolites, as active and selective green heterogeneous catalysts for the efficient oxidation of the biomass-derived levoglucosenone towards the unsaturated chiral  $\gamma$ -lactone (*S*)- $\gamma$ -hydroxymethyl- $\alpha,\beta$ -butenolide (HBO). This simple heterogeneous route to synthesize optically pure lactones derived from biomass would open up new attractive uses of metal-containing zeolites for biomass transformations.

## 2. Experimental

### 2.1. Zeolite syntheses

**2.1.1. Sn-Beta.** Sn-Beta zeolite was prepared as follows: 21.05 g of a tetraethylammonium hydroxide solution (Sigma-Aldrich, 35 wt% in water) was mixed with 20.89 g of tetraethylorthosilicate (TEOS, Sigma-Aldrich, 98 wt%) and 0.282 g of tin(IV) chloride pentahydrate (Sigma-Aldrich, 98 wt%). The mixture was stirred until the ethanol formed upon hydrolysis of TEOS was evaporated. Finally, 2.0 g of an HF solution (Sigma-Aldrich, 48 wt% in water) was added, resulting in a thick gel. The resulting gel was allowed to reach the desired concentration by controlling the water evaporation. The final gel composition was  $\text{SiO}_2/0.008 \text{ Sn}/0.54 \text{ TEAOH}/0.54 \text{ HF}/3\text{H}_2\text{O}$ . This gel was transferred to a Teflon-lined stainless steel autoclave and heated at 140 °C for 21 days in a rotary oven. The solid was recovered by filtration, extensively washed with water, and dried at 100 °C overnight. The material was calcined at 580 °C for 6 hours to remove the organic content located within the crystalline material.

**2.1.2. Zr-Beta.** Zr-Beta zeolite was prepared as follows: 21.00 g of a tetraethylammonium hydroxide solution (Sigma-Aldrich, 35 wt% in water) was mixed with 20.88 g of tetraethylorthosilicate (TEOS, Sigma-Aldrich, 98 wt%) and 0.263 g of

zirconyl chloride octahydrate (Sigma-Aldrich, 98 wt%). The mixture was stirred until the ethanol formed upon hydrolysis of TEOS was evaporated. Finally, 2.0 g of an HF solution (Sigma-Aldrich, 48 wt% in water) was added, resulting in a thick gel. The resulting gel was allowed to reach the desired concentration by controlling the water evaporation. The final gel composition was SiO<sub>2</sub>/0.008 Zr/0.54 TEOH/0.54 HF/3H<sub>2</sub>O. This gel was transferred to a Teflon-lined stainless steel autoclave and heated at 140 °C for 21 days in a rotary oven. The solid was recovered by filtration, extensively washed with water, and dried at 100 °C overnight. The material was calcined at 580 °C for 6 hours to remove the organic content located within the crystalline material.

**2.1.3. Al-Beta(OH) and Al-Beta(F).** The commercially available Al-Beta(OH) CP811 provided by P.Q. Industries was used as a Beta sample prepared in OH media. An Al-Beta sample with a much lower amount of defects, Al-Beta(F), was synthesized in fluoride media as follows: 21.04 g of a tetraethylammonium hydroxide solution (Sigma-Aldrich, 35 wt% in water) was mixed with 20.84 g of tetraethylorthosilicate (TEOS, Sigma-Aldrich, 98 wt%) and 0.363 g of aluminum isopropoxide (IPA, Sigma-Aldrich, 98 wt%). The mixture was stirred until the ethanol and isopropanol formed upon hydrolysis of TEOS and IPA were evaporated. Finally, 2.08 g of an HF solution (Sigma-Aldrich, 48 wt% in water) was added, resulting in a thick gel. The resulting gel was allowed to reach the desired concentration by controlling the water evaporation. The final gel composition was SiO<sub>2</sub>/0.033 Al/0.5 TEOH/0.5 HF/3H<sub>2</sub>O. This gel was transferred to a Teflon-lined stainless steel autoclave and heated at 140 °C for 14 days in a rotary oven. The solid was recovered by filtration, extensively washed with water, and dried at 100 °C overnight. The material was calcined at 580 °C for 6 hours to remove the organic content located within the crystalline material.

## 2.2. Characterization

Powder X-ray diffraction (PXRD) measurements were performed in a multisample Philips X'Pert diffractometer equipped with a graphite monochromator, operating at 45 kV and 40 mA, and using Cu K<sub>α</sub> radiation ( $\lambda = 0.1542$  nm).

The chemical analyses were carried out in a Varian 715-ES ICP-Optical Emission spectrometer, after solid dissolution in an HNO<sub>3</sub>-HCl-HF aqueous solution.

The morphology of the samples was studied by scanning electron microscopy (SEM) using a JEOL JSM-6300 microscope.

UV-Vis spectra were obtained with a PerkinElmer (Lambda 19) spectrometer equipped with an integrating sphere with BaSO<sub>4</sub> as the reference.

Infrared spectra were measured with a Nicolet 710 FT IR spectrometer. Pyridine adsorption-desorption experiments were performed on self-supported wafers (10 mg cm<sup>-1</sup>) of original samples previously activated at 673 K and 10<sup>-2</sup> Pa for 2 hours. After wafer activation, the base spectrum was recorded and pyridine vapour (6.5 × 10<sup>2</sup> Pa) was admitted in the vacuum IR cell and adsorbed onto the zeolite. Desorption of pyridine was performed in vacuum over three consecutive one-hour

periods of heating at 423, 523 and 623 K, each of them followed by the IR measurement at room temperature. All the spectra were scaled according to the sample weight.

Enantioselectivity evaluation of catalytic (*S*)- $\gamma$ -hydroxymethyl- $\alpha,\beta$ -butenolide (HBO) was performed firstly by chiral thin layer chromatography (Fluka, RP-18 Chiral Modified TLC), Cu<sup>2+</sup> impregnated, with a fluorescent indicator (254 nm), and secondly, by measuring the optical rotation for the target compound on a Jasco P-1030 polarimeter using the sodium yellow line (*D*) at 589 nm. Specific rotation values [ $\alpha$ ]<sub>D</sub><sup>20</sup> were calculated using the following equation:

$$\alpha = [\alpha]_D^T \times c \times l$$

[ $\alpha$ ]<sub>D</sub><sup>T</sup>: specific rotation (dm<sup>-1</sup> g<sup>-1</sup> cm<sup>3</sup>), at 20 °C; *c*: concentration is reported in g cm<sup>-3</sup>; *l*: path length (dm).

## 2.3. Catalytic tests

Levoglucosenone (95%) was purchased from Carbosynth. (*S*)- $\gamma$ -Hydroxymethyl- $\alpha,\beta$ -butenolide (98%) was purchased from Alfa-Aesar. Hydrogen peroxide (35% w/w) was purchased from Sigma-Aldrich. Acetonitrile, acetone and 1,4-dioxane were of HPLC quality grade and were acquired from Alfa-Aesar. Ultra-pure laboratory grade water (MilliQ, 18.2 megaOhms, 25 °C) was employed for HPLC analysis. All the reactants were used without further purification. Amberlyst-15 was acquired from Sigma-Aldrich.

The reaction was carried out in sealed reactors, under magnetic stirring and heating the solution at the desired temperature in an oil bath. In a typical reaction, 0.33 mmol (42 mg) of levoglucosenone was dissolved in 1 ml of 1,4-dioxane, and 0.5 mmol (48 mg) of H<sub>2</sub>O<sub>2</sub> (35% w/w in water) was added to the solution. The amount of catalyst was varied depending on the levoglucosenone/active site ratio. 10  $\mu$ l samples were collected along the reaction (by cooling down the reactor with ice) and diluted with 1.5 ml of acetonitrile. Separation of the catalyst was done by filtration (nylon 0.2  $\mu$ m syringe filters).

The experiment performed following a two-step procedure (entry 11 of Table 2) was carried out as follows: 0.33 mmol (42 mg) of levoglucosenone was dissolved in 1 ml of 1,4-dioxane, and 0.5 mmol (48 mg) of H<sub>2</sub>O<sub>2</sub> (35% w/w in water) was added to the solution. This feed was contacted with Sn-Beta catalyst (the LGO/Sn ratio was fixed at 20), and the reaction was kept at 100 °C for 4 hours. Then, the reaction solution was separated from the catalyst by filtration, and contacted with 140 mg of the acid resin Amberlyst-15 at room temperature for six hours.

The evolution of reactions was followed by HPLC, injecting 10  $\mu$ l of samples, and monitoring product formation at 220 nm. Samples from the catalytic test were analyzed by HPLC (Varian ProStar 330, equipped with a Quaternary Pump, a Rheodyne injector and a UV-Vis PDA detector), using a C18 chromatographic column (Mediterranean Sea C18, 5  $\mu$ m, 0.46 × 250 mm). A gradient elution system (0.8 ml min<sup>-1</sup>) was developed for complete separation of the reaction crude (from *t* = 0 to *t* = 5 min: H<sub>2</sub>O-acetonitrile 85% : 15%; from *t* = 5 to

$t = 10$  min: H<sub>2</sub>O–acetonitrile 90% : 10%; from  $t = 10$  to  $t = 15$  min: H<sub>2</sub>O–acetonitrile 90% : 10%; from  $t = 15$  to  $t = 20$  min: H<sub>2</sub>O–acetonitrile 85% : 15%.

### 3. Results and discussion

#### 3.1. Zeolite synthesis and characterization

Different tetrahedrally-coordinated isolated metals in zeolite frameworks perform as excellent Lewis acid active sites,<sup>14,16</sup> and isolated tin and zirconium atoms in the framework of Beta zeolite have been described as green and highly stable Lewis acid catalysts, even in aqueous media where Lewis acidity is often suppressed.<sup>1,17,21</sup> Beta zeolite is a very open tri-directional large pore molecular sieve with channel openings between 6.5 and 7 Å.<sup>22</sup> In this sense, Sn-Beta and Zr-Beta could be adequate candidates for their use as catalysts in the oxidation of levoglucosone to  $\gamma$ -lactone (*S*)- $\gamma$ -hydroxymethyl- $\alpha,\beta$ -butenolide (HBO), because, on the one hand, metal centers would introduce the Lewis acidity required in the reaction, and on the other hand, their pore size would allow the diffusion of the reactants and products involved in the reaction.

Sn-Beta and Zr-Beta were prepared with the same Si to metal ratio (Si/M = 125, see the Experimental section for details). Both materials show the characteristic powder X-ray diffractogram (PXRD) of Beta zeolite (see Fig. 3), and chemical analyses indicate that the real Si/M ratios in the resulting solids are similar to the gel ratios (Si/Sn = 114, and Si/Zr = 127, for Sn-Beta and Zr-Beta, respectively, see Table 1). These two metallozeolites show comparable crystal sizes between 1 and 3  $\mu\text{m}$  (see SEM images C and D in Fig. 4). Sn-Beta and Zr-Beta were also studied by UV-Vis spectroscopy to identify if Sn and Zr species have been inserted in framework positions. As observed in Fig. 5, Sn-Beta presents a band centered at 200 nm, and Zr-Beta shows a band centered at 215 nm, which have been previously assigned to the characteristic UV radiation absorption of these metals in zeolitic framework positions.<sup>23</sup>

As a general description, the introduction of aluminum atoms in the framework of zeolites creates negative charges in

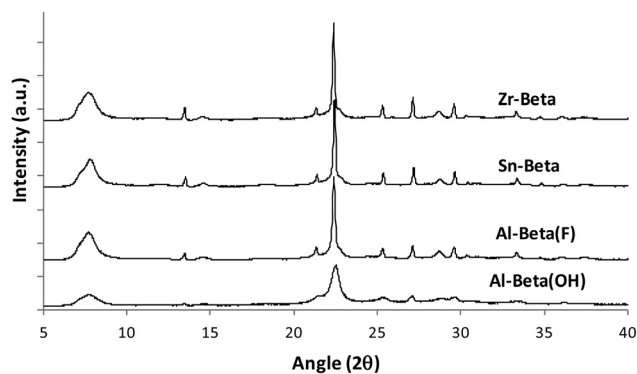


**Fig. 3** Powder X-ray diffractograms (PXRD) of the different metal-containing Beta zeolites in their calcined form.

**Table 1** Chemical analyses and crystal size of the different metal-containing zeolites

Sample	Heteroatom	Si/Het. <sup>a</sup>	Crystal size <sup>b</sup> ( $\mu\text{m}$ )	BET surface area <sup>c</sup> ( $\text{m}^2 \text{g}^{-1}$ )	Micropore volume <sup>c</sup> ( $\text{cm}^3 \text{g}^{-1}$ )
Al-Beta(OH)	Al	13	0.1–0.2	594	0.18
Al-Beta(F)	Al	33	0.8–2	505	0.22
Sn-Beta	Sn	114	1–2	490	0.21
Zr-Beta	Zr	127	1–3	474	0.20

<sup>a</sup> Measured by ICP. <sup>b</sup> Obtained from SEM. <sup>c</sup> Acquired from N<sub>2</sub> adsorption measurements.

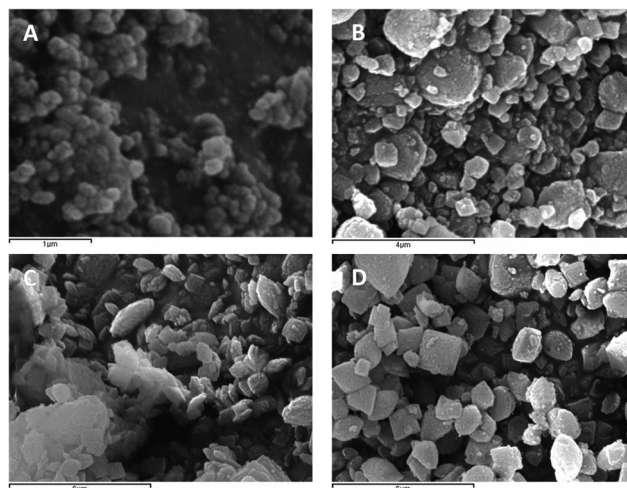


**Fig. 4** Scanning electron microscopy (SEM) images of: (A) Al-Beta(OH), (B) Al-Beta(F), (C) Sn-Beta, and (D) Zr-Beta.

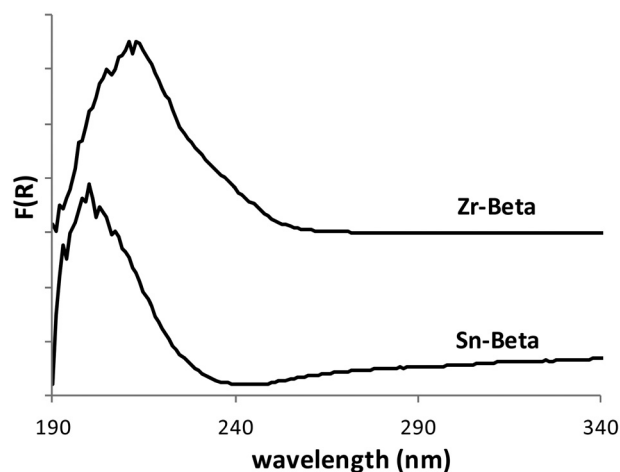


**Fig. 5** UV-Vis spectra of Sn-Beta and Zr-Beta.

the structure, which are primarily balanced by protons, making Al-containing zeolites extraordinary Brønsted acid materials.<sup>24</sup> In this sense, two different Al-Beta materials showing Brønsted acidity were selected for comparing their activity in the oxidation of LGO with the Lewis acid heterogeneous catalysts. On the one hand, the commercially

available Beta CP811 provided by P.Q. Industries [named here Al-Beta(OH)], which presents a Si/Al ratio of 13 and a very small crystal size (~100–150 nm, see Fig. 4A), and, on the other hand, an Al-Beta zeolite synthesized in fluoride media, Al-Beta(F), with a crystal size comparable to those of Sn- and Zr-Beta, were prepared and tested as catalysts (see the Experimental section for details, Fig. 4 and Table 1).

### 3.2. Catalytic tests: “one-pot” selective oxidation of levoglucosenone

The levoglucosenone oxidation experiments were performed in 2 ml reactors at 100 °C using H<sub>2</sub>O<sub>2</sub> as an oxidant and dioxane as a solvent (see the Experimental section for details). The amount of each catalyst introduced in the reaction was varied keeping the levoglucosenone/metal active site molar ratio (LGO/M) constant at 50. The reaction was followed by HPLC. From the preliminary screening results summarized in Table 2, it can be observed that Al-Beta(F), Sn-Beta and Zr-Beta are very active catalysts for LGO oxidation, with conversions higher than 90% after 4 hours of reaction. In all cases, the formil-ester product (FBO) is first formed, and later transformed to the unsaturated chiral  $\gamma$ -lactone (*S*)- $\gamma$ -hydroxymethyl- $\alpha,\beta$ -butenolide (HBO). The selectivity towards desired HBO is higher for Al-Beta(F) than for Sn-Beta and Zr-Beta, after 4 and 20 hours (see entries 4, 5, and 6 in Table 2), but the overall yield to both products (FBO + HBO) is much lower for the former (*i.e.* 62% for Al-Beta(F) *versus* 87% and 89% for Zr-Beta and Sn-Beta, respectively after 20 h). In this sense, the Brønsted acidity of Al-Beta(F) would favor the hydrolysis of the formil ester FBO towards HBO but, at the same time, this chiral sugar could also be converted to other by-products, such

as furan-derivatives in the presence of Al-Beta(F). Then, in order to see if HBO remains stable in the presence of Al-Beta(F), a blank experiment was performed, and the result given in entry 7, Table 2, clearly reveals that 25% of HBO is degraded after 20 hours of reaction.

At this point, it is important to comment on the relevant catalytic differences observed between Al-Beta(OH) and Al-Beta(F) (entries 3 and 4 in Table 2). Although both samples present Brønsted acidity, Al-Beta(F) shows much higher activity and selectivity to FBO and HBO. Those two samples were characterized by *in situ* infrared study of pyridine adsorption/desorption in order to see the acidity of the zeolites. Al-Beta(OH) and Al-Beta(F) show an IR spectrum band at 1545 cm<sup>-1</sup>, which has been assigned to protonated pyridine and, therefore, to Brønsted acid sites in the zeolites (see Fig. 6). It can be seen that the 1545 cm<sup>-1</sup> IR band of the pyridine adsorbed after evacuation at 150 °C is more intense for Al-Beta(OH) than Al-Beta(F), in clear agreement with the lower Si/Al ratio in the former. On the other hand, Al-Beta(OH) zeolite also shows much more intense IR spectra bands at 1452 and 1622 cm<sup>-1</sup> than Al-Beta(F). These two bands are associated with pyridine coordinated to Lewis acid sites that can be related to the presence of extra-framework aluminum. Indeed, it is believed that Lewis acidity in Al-containing zeolitic materials is generated by extra-framework octahedral aluminum species. Therefore, if we assume that the above described reaction must occur through a Lewis acid mechanism, the lower activity of Al-Beta(OH) when compared to Al-Beta(F) cannot be explained. However, it has been described in the literature that some Al-Beta materials are active for Lewis acid based reactions, such as Meerwein-Ponndorf-Verley (MPV).<sup>14a,25</sup> Van Bekkum *et al.* concluded that

**Table 2** Results of the oxidation of levoglucosenone using different metal-containing zeolites. Reaction conditions: 0.33 mmol LGO, 0.5 mmol H<sub>2</sub>O<sub>2</sub>, 1 ml of solvent at given temperatures and LGO/metal ratios

Entry	Catalyst	LGO/metal	Solvent	<i>T</i> (°C)	<i>t</i> (h)	Conversion	<i>S</i> <sub>FBO</sub>	<i>S</i> <sub>HBO</sub>	<i>S</i> <sub>TOTAL</sub>
1	—	—	Dioxane	100	4	3	0	0	0
2	Si-Beta	—	Dioxane	100	4	9	0	0	0
3	Al-Beta(OH)	50	Dioxane	100	4	63	39	12	51
				100	20	89	8	33	41
4	Al-Beta(F)	50	Dioxane	100	4	97	45	30	75
				100	20	100	5	57	62
5	Zr-Beta	50	Dioxane	100	4	92	67	23	90
				100	20	98	40	47	87
6	Sn-Beta	50	Dioxane	100	4	91	72	24	96
				100	20	100	41	48	89
7	Al-Beta(F)	50 (HBO) <sup>d</sup>	Dioxane	100	4	11	—	—	—
				100	20	25	—	—	—
8	Al-Beta(F)	50	Dioxane	80	20	97	45	44	89
				80	48	99	2	69	71
9	Sn-Beta + Al-Beta(F)	50 (Sn)-200 (Al) <sup>b</sup>	Dioxane	100	4	95	61	26	87
				100	20	100	18	59	77
10	Sn-Beta	20	Dioxane	100	4	98	45	50	95
				100	20	100	12	75	87
11	Sn-Beta Amberlyst-15 <sup>c</sup>	—	Dioxane	100	4	97	52	44	96
				R.T.	6	99	2	89	91
12	Sn-Beta	50	Acetonitrile	100	4	62	57	7	64
13	Sn-Beta	50	Methanol	100	4	95	0	55	55

<sup>a</sup> HBO/Al ratio. <sup>b</sup> LGO/Sn and LGO/Al ratios of 50 and 200, respectively. <sup>c</sup> 140 mg of the commercial acid resin Amberlyst-15.

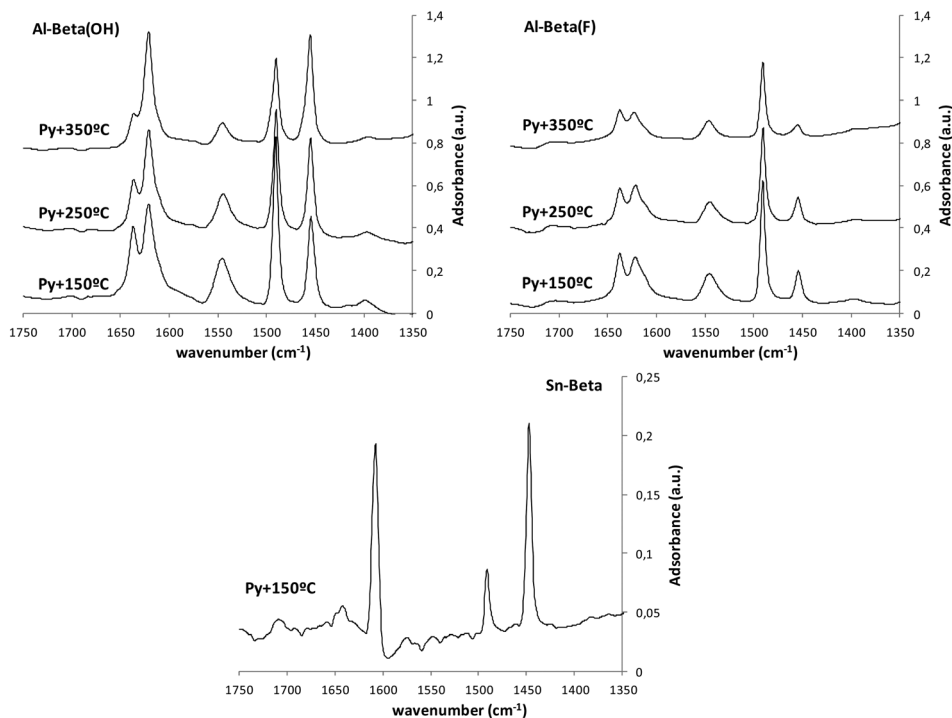


**Fig. 6** Transmission FTIR spectra in the stretching C–C region of the different metal-containing zeolites after adsorbing pyridine followed by desorption at 150, 250, and 350 °C.

extra-framework aluminum species are inactive in the MPV reaction, and alternatively proposed that the active sites are octahedrally coordinated framework aluminums, connected with four bonds to the framework, one water molecule and a hydronium ion.<sup>25</sup> Unfortunately, this specific aluminum site was not unambiguously observed by Van Bekkum *et al.*,<sup>25</sup> but their description would explain the results we have obtained for the two different Al-Beta materials in the levoglucosenone oxidation.

As has been introduced above, Al-Beta(F) zeolite is active in the LGO oxidation when the reaction is performed at 100 °C, but unfortunately undesired degradation reactions also occur affecting the total selectivity of FBO and HBO. In attempts to reduce the undesired pathways, a new experiment using Al-Beta(F) at 80 °C is carried out. After 20 hours, levoglucosenone is almost fully converted (see entry 8 of Table 2) and, interestingly, competitive degradation reaction is highly prevented ( $S_{\text{TOTAL}} = 89\%$ ) but the hydrolysis step of the formil ester FBO to HBO is very slow. After 48 hours of reaction, the selectivity to HBO is almost 70%.

Sn-Beta performs better than the other metallozeolites in terms of total yield to FBO and HBO at 100 °C with very high selectivities to these products (see entry 6 of Table 2). However, after 20 hours of reaction, the selectivity to the desired HBO is still low (see Fig. 7A). In order to increase the hydrolysis of the formil ester to HBO when Sn-Beta (LGO/Sn = 50) is used as a catalyst, we decided to combine Sn-Beta with Al-Beta(F), keeping the LGO/Sn ratio at 50 and the LGO/Al ratio at 200. Using this combination of Lewis acid sites with a small amount of

Brönsted acid sites, the HBO yield improves up to 59%, but at the same time, the total yield to FBO plus HBO drops when compared to Sn-Beta (see  $S_{\text{TOTAL}}$  in entries 6 and 9 of Table 2). That means that although the Brönsted acidity introduced in the reaction mixture is very low, HBO is still being degraded to other by-products on the Brönsted acid sites.

The oxidation catalytic profile of levoglucosenone using Sn-Beta (LGO/Sn = 50, see Fig. 7A) reveals that Lewis acid sites introduced by isolated tin centers in framework positions are able to perform the hydrolysis of the formil ester FBO product to HBO. This hydrolysis rate is slower when compared to Brönsted acid Al-Beta(F), but at the same time, the presence of undesired competitive degradation reactions catalyzed by Brönsted acid sites are prevented with Sn-Beta. To ensure the absence of Brönsted acid sites in Sn-Beta, this material was characterized by *in situ* infrared study of pyridine adsorption/desorption, and as seen in Fig. 6, the unique bands present in the spectrum after desorption at 150 °C are those associated with Lewis acid sites (1452 and 1622  $\text{cm}^{-1}$ ). Then, it could be predicted that if the amount of Sn-Beta is increased in the reaction mixture, the hydrolysis rate of FBO to HBO will also be increased, while the presence of undesired competitive reactions should mostly be prevented. Having that in mind, a new experiment using Sn-Beta as a catalyst is performed fixing the LGO/Sn ratio at 20. As seen in Fig. 7B and Table 2 entry 10, the hydrolysis rate to HBO is notoriously increased, achieving a HBO yield of 75% after 20 hours. Interestingly, the total yield to the main products (FBO + HBO) is fixed after increasing the catalytic active sites in the reaction (compare entries 6 and 10

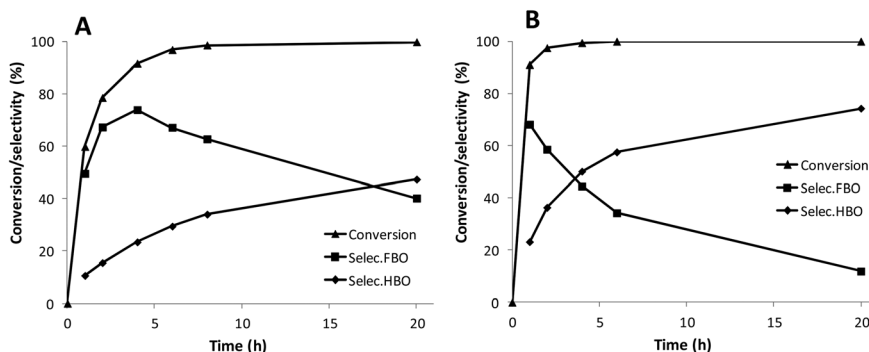


**Fig. 7** Levoglucosenone (LGO) oxidation reaction profiles and product distributions as a function of time when Sn-Beta is used as a catalyst with a LGO/Sn ratio of 50 (A) and 20 (B). Reaction conditions: 0.33 mmol LGO, 0.5 mmol H<sub>2</sub>O<sub>2</sub>, 1 ml dioxane at 100 °C.

in Table 2). This result is interesting since the previous yield described in homogeneous catalysis using organic peroxides was 65%.<sup>11</sup> Furthermore, the efficiency of H<sub>2</sub>O<sub>2</sub> was measured, obtaining values higher than 90% after 1 and 4 hours of reaction.

In addition to dioxane, other protic and aprotic solvents with similar polarities were studied using Sn-Beta as a catalyst. As seen in Table 2, the oxidation of LGO in acetonitrile shows lower activity and very low selectivity to HBO (entry 12), while in methanol the activity is similar to dioxane but the total selectivity to FBO and HBO is low (entry 13).

### 3.3. Catalytic tests: “two-step” selective oxidation of levoglucosenone

The HBO yield can be increased from 75% to 90% by designing a very simple “two-step” procedure using a combination of Sn-Beta and the acid resin Amberlyst-15 (see entry 11 of Table 2 and the Experimental section). The LGO feed is first contacted with the Sn-Beta catalyst at 100 °C for 4 hours, and later, the catalyst is separated from the reaction solution by filtration. At that moment, the LGO conversion is almost complete (97%), and the yield to the intermediate formil butenolide (FBO) is close to 50%. We have seen above that for a longer time using Sn-Beta as a catalyst favors the FBO transformation into HBO (see entry 10 in Table 2), but the hydrolysis rate is low. This hydrolysis rate can be increased by using Brønsted acid catalysts, such as Al-Beta zeolites, but undesired by-products are formed under those elevated temperatures. To avoid this degradation, we propose as an alternative the use of an acid resin, such as commercially available Amberlyst-15. This acid resin shows less diffusion problems than Al-Beta zeolites and the hydrolysis step of FBO to HBO could be performed at lower temperatures avoiding undesired degradation reactions. As seen in entry 11 of Table 2, Amberlyst-15 performs the complete hydrolysis of the remaining FBO at room temperature after 6 hours, achieving up to 90% yield of desired HBO.

### 3.4. (S)-γ-Hydroxymethyl-α,β-butenolide characterization

Since the desired product is the chiral γ-lactone (S)-γ-hydroxymethyl-α,β-butenolide (HBO), an additional characterization has been performed for studying its optical purity. From the

crude obtained after reacting levoglucosenone with Sn-Beta for 20 hours in dioxane (entry 10 in Table 2), HBO product was isolated and purified in a column. On the one hand, a special thin-layer chromatography (TLC) plate for enantiomeric chiral analysis (see the Experimental section) was used to evaluate the optical purity of HBO using acetonitrile-CH<sub>2</sub>Cl<sub>2</sub> (10 : 90 v/v) as the mobile phase. Only one compound was observed in the TLC plate, with the same R<sub>f</sub> = 0.19 as the commercial enantiomeric pure sample of HBO. On the other hand, the optical purity of the isolated HBO product after reaction was also determined by measuring the specific rotation  $[\alpha]_D^{25}$  (see the Experimental section for details) for the HBO-catalytic product. The achieved value  $[\alpha]_D^{25} = -114.56$  for the isolated HBO was in agreement with the value obtained ( $[\alpha]_D^{25} = -117.01$ ) for the commercially available γ-lactone (S)-γ-hydroxymethyl-α,β-butenolide, measured under the same experimental conditions. From both the experimental results, it could be said that S-enantiomer of HBO is formed in more than 95%, by reacting LGO in the presence of Sn-Beta catalyst.

### 3.5. Catalyst stability

Finally, the stability of Sn-Beta was studied. The catalyst was filtered and washed with acetone after the catalytic test for its re-use. As seen in Table 3, the recycled catalyst shows a slightly lower activity than fresh Sn-Beta after 1 hour of reaction, and it also shows lower selectivities to HBO after 1 and 4 hours of reaction. The recovered solid from the 1st catalytic cycle was calcined in air at 550 °C for 6 h. This calcined catalyst was tested in the levoglucosenone oxidation, and as observed in

**Table 3** Study of the Sn-Beta stability after different catalytic cycles

	Si/Sn <sup>a</sup>	LGO/Sn	Time (h)	Conversion	S <sub>HBO</sub>
Fresh	117	20	1	90	22
			4	99	49
1st Cycle	122	20	1	71	15
			4	98	31
2nd Cycle <sup>b</sup>	120	20	1	86	19
			4	99	42

<sup>a</sup> Measured by ICP after each experiment. <sup>b</sup> Catalyst recovered from the 1st cycle was calcined in air at 550 °C for 6 h.

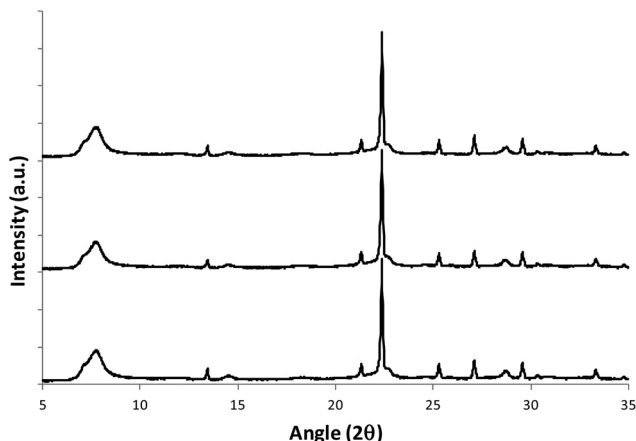


Fig. 8 Powder X-ray diffractograms (PXRD) of the Sn-Beta catalyst after each catalytic cycle (see Table 3).

Table 3, the initial activity and the yield to the desired HBO product are most recuperated. This result indicates that the decrease in activity and selectivity after the first cycle could be attributed to the catalyst poisoning by organic deposits. Moreover, PXRD patterns (see Fig. 8) and chemical analyses (see the Si/Sn ratio in Table 3) clearly reveal the structural and chemical stabilities of the Sn-Beta catalyst after each catalytic cycle.

## 4. Conclusions

Efficient heterogeneous catalysts based on metal-containing zeolites have been applied to the oxidation of levoglucosenone towards the unsaturated chiral  $\gamma$ -lactone (*S*)- $\gamma$ -hydroxymethyl- $\alpha,\beta$ -butenolide (HBO) using  $H_2O_2$  as a green oxidant. This catalytic route is of interest since levoglucosenone is one of the major products obtained from biomass fast pyrolysis, and the chiral  $\gamma$ -lactone HBO is a high-valuable chemical with applications in flavors and biomedicine. Sn-Beta performs better than other metalloaluminates, achieving HBO yields of up to 75% in a “one-pot” system. This value is higher than that previously reported with homogeneous catalysts using organic peracids as oxidants (65%). The HBO yield is increased up to 90% if Sn-Beta catalyst is combined with an acid resin in a “two-step” procedure.

## Acknowledgements

This work has been supported by the Spanish Government MINECO through Consolider Ingenio 2010-Multicat and MAT2012-37160, and by UPV through PAID-06-11 (n.1952). Manuel Moliner also acknowledges “Subprograma Ramon y Cajal” for contract RYC-2011-08972. ITQ thanks the “Program Severo Ochoa” for financial support.

## References

- 1 A. Corma, S. Iborra and A. Velty, *Chem. Rev.*, 2007, **107**, 2411.
- 2 G. W. Huber, S. Iborra and A. Corma, *Chem. Rev.*, 2006, **106**, 4044.
- 3 (a) M. S. Miftakhov, F. A. Valeev and I. N. Gaisina, *Russ. Chem. Rev.*, 1994, **63**, 869; (b) A. V. Bridgwater, D. Meier and D. Radlein, *Org. Geochem.*, 1999, **30**, 1479; (c) Q. Lu, W. M. Xiong, W. Z. Li, Q. X. Guo and X. F. Zhu, *Bioresour. Technol.*, 2009, **100**, 4871.
- 4 (a) F. Shafizadeh, R. H. Furneaux, T. T. Stevenson and T. G. Cochran, *Carbohydr. Res.*, 1978, **61**, 519; (b) G. Dobeles, T. Dizhbite, G. Rossinskaja, G. Telysheva, D. Mier, S. Radtke and O. Faix, *J. Anal. Appl. Pyrolysis*, 2003, **68–69**, 197; (c) J. Zandersons, A. Zhurinsk, G. Dobeles, V. Jurkane, J. Rizhikovs, B. Spince and A. Pazhe, Feasibility of broadening the feedstock choice for levoglucosenone production by acid pre-treatment of wood and catalytic pyrolysis of the obtained lignocellulose, *J. Anal. Appl. Pyrolysis*, 2013, DOI: 10.1016/j.jaap.2013.01.014.
- 5 J. Jae, G. A. Tompsett, A. J. Foster, K. D. Hammond, S. M. Auerbach, R. F. Lobo and G. W. Huber, *J. Catal.*, 2011, **279**, 257.
- 6 J. A. Marshall, *An improved preparation of levoglucosenone from cellulose*, Iowa State University, Master thesis, 2008.
- 7 (a) V. L. Budarin, P. S. Shuttleworth, J. R. Dodson, A. J. Hunt, B. Lanigan, R. Marriott, K. J. Milkowski, A. J. Wilson, S. W. Breeden, J. Fan, E. H. K. Sin and J. H. Clark, *Energy Environ. Sci.*, 2011, **4**, 471; (b) X. Hu, L. Wu, Y. Wang, D. Mourant, C. Lievens, R. Gunawan and C. Z. Li, *Green Chem.*, 2012, **14**, 3087.
- 8 (a) K. Tomioka, T. Ishiguro and K. Koga, *J. Chem. Soc., Chem. Commun.*, 1979, 652; (b) D. Enders, V. Lausberg, G. Del Signore and O. M. Berner, *Synthesis*, 2002, 515.
- 9 E. Takashi, M. Katsuya, Y. Hajime, K. Koseki, H. Kawakami and H. Matsushita, *Heterocycles*, 1990, **31**, 1585.
- 10 (a) H. Hawakami, T. Ebata, K. Koseki, K. Statsumoto, H. Matsushita, Y. Naoi and K. Itoh, *Heterocycles*, 1990, **31**, 2041; (b) R. Flores, A. Rustullet, R. Alibes, A. Alvarez-Larena, P. de March, M. Figueredo and J. Font, *J. Org. Chem.*, 2011, **76**, 5369; (c) A. Diaz-Rodriguez, Y. S. Sanghvi, S. Fernandez, R. F. Schinazi, E. A. Theodorakis, M. Ferrero and V. Gotor, *Org. Biomol. Chem.*, 2009, **7**, 1415.
- 11 K. Koseki, T. Ebata, H. Kawakami, H. Matsushita, Y. Naoi and K. Itoh, *Heterocycles*, 1990, **31**, 423.
- 12 F. Shafizadeh, R. H. Furneaux and T. T. Stevenson, *Carbohydr. Res.*, 1979, **71**, 169.
- 13 A. Corma, L. T. Nemeth, M. Renz and S. Valencia, *Nature*, 2001, **412**, 423.
- 14 (a) A. Corma, M. E. Domine, L. Nemeth and S. Valencia, *J. Am. Chem. Soc.*, 2002, **124**, 3194; (b) M. Boronat, P. Concepcion, A. Corma, M. Renz and S. Valencia, *J. Catal.*, 2005, **234**, 111; (c) A. Corma, S. Iborra, M. Mifsud, M. Renz and M. Susarte, *Adv. Synth. Catal.*, 2004, **346**, 257.
- 15 M. Boronat, A. Corma and M. Renz, *J. Phys. Chem. B*, 2006, **110**, 21168.
- 16 Y. Roman-Leshkov and M. E. Davis, *ACS Catal.*, 2011, **1**, 1566.

- 17 (a) M. Moliner, Y. Roman-Leshkov and M. E. Davis, *Proc. Natl. Acad. Sci. U. S. A.*, 2010, **107**, 6164; (b) Y. Roman-Leshkov, M. Moliner, J. A. Labinger and M. E. Davis, *Angew. Chem., Int. Ed.*, 2010, **49**, 8954.
- 18 (a) E. Nikolla, Y. Roman-Leshkov, M. Moliner and M. E. Davis, *ACS Catal.*, 2011, **1**, 408; (b) C. M. Lew, N. Rajabbeigi and M. Tsapatsis, *Ind. Eng. Chem. Res.*, 2012, **51**, 5364.
- 19 M. S. Holm, S. Saravanamurugan and E. Taarning, *Science*, 2010, **328**, 602.
- 20 W. R. Gunther, Y. Wang, Y. Ji, V. K. Michaelis, S. T. Hunt, R. G. Griffin and Y. Román-Leshkov, *Nat. Commun.*, 2012, **3**, 1109.
- 21 (a) A. Corma, M. E. Domine and S. Valencia, *J. Catal.*, 2003, **215**, 294; (b) A. Corma and M. Renz, *Chem. Commun.*, 2004, 550; (c) A. Corma and M. Renz, *Angew. Chem., Int. Ed.*, 2007, **46**, 298.
- 22 M. M. J. Treacy and J. M. Newsam, *Nature*, 1988, **332**, 249.
- 23 (a) C. C. Chang, Z. Wang, P. Dornath, H. J. Cho and W. Fan, *RSC Adv.*, 2012, **2**, 10475; (b) T. Tatsumi, P. Wu and K. Tsuji, *U.S. Patent 7326401*, 2008.
- 24 (a) J. A. Rabo, *Catal. Rev. Sci. Eng.*, 1981, **23**, 293; (b) A. Corma, *Chem. Rev.*, 1997, **97**, 2373.
- 25 P. J. Kunkeler, B. J. Zuurdeeg, J. C. van der Waal, J. A. van Bokhoven, D. C. Koningsberger and H. van Bekkum, *J. Catal.*, 1998, **180**, 234.